European Review for Medical and Pharmacological Sciences 2018; 22: 7148-7155

Autologous oxygen release nano bionic scaffold composite miR-106a induced BMSCs enhances osteoblast conversion and promotes bone repair through regulating BMP-2

M.-H. SUN[1], W.-J. WANG[1], Q. LI[2], T. YUAN[1], W.-J. WENG[1]

[1]Department of Joint Surgery, The Affiliated Drum Tower Hospital of Nanjing University Medical School, Nanjing, Jiangsu, China
[2]Department of Clinical Medicine of Chinese and Western Medicine Integration, Nanjing University of Chinese Medicine, Nanjing, Jiangsu, China

Abstract. – OBJECTIVE: Suitable seed cells and selection of bioactive scaffold materials are the main research contents of bone tissue engineering. It was showed that autologous oxygen release nano bionic scaffold could promote the osteogenic differentiation of bone marrow mesenchymal stem cells (BMSCs). The role of microRNA-106a (miR-106a) in regulating BMSCs differentiation has not been reported. We intend to investigate the role of autologous oxygen release nano bionic scaffold composite miR-106a in inducing BMSCs constructing tissue engineering bone.

MATERIALS AND METHODS: Rat BMSCs were isolated and transfected by using miR-106a scramble or miR-106a inhibitor. Healthy male Sprague-Dawly (SD) rats were randomly divided into three groups, including bone fracture group established as rat tibial fracture model, negative control group implanted by autologous oxygen release nano bionic scaffold composite miR-106a scramble BMSCs, and miR-106a inhibitor group implanted by autologous oxygen release nano bionic scaffold composite miR-106a inhibitor BMSCs. Callus growth was observed. Alkaline phosphatase (ALP) activity was detected. Bone morphogenetic protein 2 (BMP-2) expression was tested by Real-time PCR (RT-PCR) and Western blot assay. Collagen II production was determined by RT-PCR.

RESULTS: Autologous oxygen release nano bionic scaffold composite BMSCs significantly increased local bone mineral density, promoted callus healing, facilitated ALP secretion, elevated collagen II expression, and up-regulated BMP-2 mRNA and protein levels compared with fracture group ($p<0.05$). Autologous oxygen release nano bionic scaffold composite miR-106a induced BMSCs exhibited more significant effect on bone repair ($p<0.05$).

CONCLUSIONS: Autologous oxygen release nano bionic scaffold composite miR-106a induced BMSCs enhanced osteoblast conversion and promoted bone repair through regulating BMP-2.

Key Words:
Autologous oxygen release nano bionic scaffold, Bone marrow mesenchymal stem cell, miR-106a, Tissue engineering bone, BMP-2.

Introduction

Following the rapid development of life science technology and engineering, tissue engineering technology has been widely used in clinical practice[1]. Tissue engineering technology combines biology principle and biological engineering technology, isolated and cultured seed cells, and selected biological activity material. It may make new tissue engineering material to undertake new tissue function, thus providing basis for damaged organ repair, alternation, and improvement[2,3]. In the process of fracture and bone defect occurrence, regenerative ability is restricted because of blood supply and lymph circumfluence deficiency. Therefore, tissue-engineering technology is indispensable for the repair and healing of fracture[4,5]. Bone mesenchymal stem cells (BMSCs) are derived from bone marrow and mainly exist in marrow stroma cells. It is a kind of multi-potential stem cells that can differentiate to bone, cartilage, and adipose tissue. Under suitable stimulus, it can further form muscle, fat, bone, cartilage, and even ligament tissue[6,7]. *In vitro* cultivation can induce BMSCs differentiation into osteo-

Corresponding Author: Wenjie Weng, MD; e-mail: drwengwenjie@hotmail.com

blasts that are similar to hydroxyapatite crystal. BMSCs have been observed with good osteogenic capability in animal model[8,9]. In the study of bone tissue engineering, another conundrum is the selection of suitable cell scaffold material. Cell scaffold material selection mainly focuses on biological material, biological ceramic material, polymer material, and composite material[10,11]. Autologous oxygen release nano bionic scaffold is a type of new scaffold material that adds chitosan into hexafluoroisopropanol. After low temperature stirring to form chitosan solution, it was mixed with nano-hydroxyapatite and peroxide. After sonification and paraffin mold preparation, it forms biological scaffold after freeze drying[12,13]. Autologous oxygen release nano bionic scaffold can promote cartilage cell aggregation and adhesion, as well as BMSCs osteogenesis[14,15]. It was found that microRNA (miRNA) plays an important role in regulating BMSCs differentiation. However, there is still lack of report about the role of miR-106a in BMSC[16,17]. We investigated the role of autologous oxygen release nano bionic scaffold composite miR-106a in inducing BMSCs constructing tissue-engineering bone.

Materials and Methods

Experimental Animals

A total of 60 healthy male Sprague-Dawly (SD) rats (Provided by Nanjing University Medical School) at two months old and weighted 250 ± 20 g were purchased from Experimental Animal Center and raised in Specific-Pathogen-Free (SPF) grade Experimental Animal Center. The raising condition contained temperature at 21 ± 1°C, relative humidity at 50-70%, and 12 h day/night cycle. Rats were used for all experiments, and all procedures were approved by the Animal Ethics Committee of The Affiliated Drum Tower Hospital of Nanjing University Medical School (Nanjing, Jiangsu, China).

Main Reagents and Instruments

Pentobarbital sodium and lidocaine were bought from Shanghai GenePharma Co. Ltd. (Shanghai, China). L-Dulbecco's modified eagle medium (L-DMEM) was purchased from Gibco (Grand Island, NY, USA). Alkaline phosphatase (ALP) activity detection kit was derived from R&D systems Inc. (Minneapollis, MN, USA). Polyvinylidene difluoride (PVDF) membrane was purchased from Pall Life Sciences (Covina, CA, USA). *Ethylene diamine tetraacetic acid* (EDTA) was obtained from HyClone (South Logan, UT, USA). Western blot related reagents were provided by Beyotime Biotech. (Shanghai, China). Enhanced chemiluminescence (ECL) reagent was purchased from Amersham Biosciences (Little Chalfont, Buckinghamshire, UK). Rabbit anti mouse monoclonal antibodies and goat anti rabbit horseradish peroxidase (HRP) labeled IgG secondary antibody were obtained from Cell Signaling Technology (Danvers, MA, USA). CD26 and CD44 rabbit anti mouse polyclonal antibodies were provided by Cell Signaling Technology (Danvers, MA, USA). Glyceric acid phosphate sodium, dexamethasone, and ascorbic acid were bought from Sigma-Aldrich (St. Louis, MO, USA). MiR-106a scramble and inhibitor were purchased from Shanghai GenePharma Co. Ltd. (Shanghai, China). RNA extraction kit and reverse transcription kit were purchased from Axygen (Tewksbury, MA, USA). ABI 7700 Fast real-time PCR amplifier was derived from ABI (Foster City, CA, USA). DNA amplifier was got from PE Gene Amp PCR System 2400 (PE Gene Applied Biosystems, Foster, CA, USA). Labsystem version 1.3.1 microplate reader was provided by BD Biosciences (Franklin Lakes, NJ, USA). King-8000 bone sonometer was purchased from Jinchangyu (Xi'an, China).

Rat BMSCs Isolation and Identification

The femur and tibia were isolated from SD rat and moved to sterile plate. The bone marrow was extracted using injection syringe and added to 10 ml serum free medium. After re-suspended in 3 ml phosphate-buffered saline (PBS), the cells were centrifuged at 1000 r/min for 10 min to remove supernatant and fat. The cells were further added to equal volume of lymphocyte separation medium and centrifuged at 2500 r/min and room temperature for 25 min. Next, BMSCs were cultured in L-DMEM medium containing 10% FBS and 1% penicillin-streptomycin at 37°C and 5% CO_2. The medium was changed after 48 h to remove unattached cells. The cells were identified and passaged when cell fusion reached 80%. They were washed by PBS and fixed in 4% paraformaldehyde. Next, the cells were incubated in CD29 and CD44 rabbit anti rat polyclonal antibodies (1:100) at 4°C overnight. Next, the cells were incubated in goat anti rabbit FITC labeled secondary antibody at room temperature. At last, the cells were observed under the fluorescent microscope. BMSCs in 2^{nd}-5^{th} generation were used for the following experiment.

MiR-106a Inhibitor Liposome Transfection

MiR-106a scramble and inhibitor were transfected to BMSCs in logarithmic phase. The sequences used were as follows. MiR-106a scramble, 5'-UGUUACAACAGUGUCGUGGA-3'; miR-106a inhibitor, 5'-ACCGGUCUGUUUGAGAGA-3'. MiR-106a inhibitor and negative control were added to 200 μl serum free medium and incubated at room temperature for 15 min. Then lipo2000 was mixed with miR-106a inhibitor or negative control and incubated at room temperature for 30 min. Next, the mixture was added to cells in serum free medium and cultured at 37°C and 5% CO_2 for 6 h. After changing the medium, the cells were further cultured for 48 h for the following experiments.

Autologous Oxygen Release Nano Bionic Scaffold Preparation

Hexafluoroisopropanol was added with chitosan at low temperature to form solution occupying 40% of total mass[12,13]. Next, it was mixed with nano-hydroxyapatite and peroxide, accounting for 60% of total mass. After sonification, it was cross linked with genipin and put into the mold to prepare sample. It was frozen, separated and dried to remove paraffin-using n-hexane. At last, it formed autologous oxygen release nano bionic scaffold after freeze-drying.

Rat Fracture Model Establishment and Grouping

The rat was anesthetized by 10% chloral hydrate at 0.3 g/kg and the left leg was sterilized. The tibia was sawed-off at tuberosity and washed by normal saline. The rats were randomly divided into three groups, including bone fracture group, negative control group implanted by autologous oxygen release nano bionic scaffold composite 1×10^5 miR-106a scramble BMSCs, and miR-106a inhibitor group implanted by autologous oxygen release nano bionic scaffold composite 1×10^5 miR-106a inhibitor BMSCs. At last, the incision was sutured and the rat received penicillin injection for 3 days to prevent infection.

Sample Collection

At 6 weeks after modeling, a total of 2 ml blood were extracted from portal vein and centrifuged at 3000 r/min for 15 min. The rat was executed and the tissues at 0.6 cm from the fracture part were extracted.

Callus Growth

After euthanasia, the bone mineral density (BMD) of the fracture part was tested by bone sonometer. The BMD was detected at 2.0 mm×1.5 mm region around the fracture part.

ALP Content Detection

ALP content was tested using the detection kit. The cells were centrifuged at 1000 r/m for 10 min and added with Triton-X 100. At last, the cells were tested at 520 nm to calculate ALP content.

Real-Time PCR

Total RNA was extracted from the tissue by TRIzol and reverse transcribed to cDNA. The primers were designed using Primer 6.0 software and synthesized by Invitrogen (Table I). Real-time PCR was performed at 56°C for 1 min, followed by 35 cycles of 92°C for 30 s, 58°C for 45 s, and 72°C for 35 s. Glyceraldehyde-3-phosphate dehydrogenase (GAPDH) was selected as internal reference. The relative expression of mRNA was calculated by $2^{-\Delta Ct}$ method.

Western Blot

The bone tissue was added with Roswell Park Memorial Institute-1640 (RPMI-1640) and cracked on ice for 15-30 min. Next, the tissues were treated by ultrasound at 5 s for 4 times and centrifuged at 10000 ×g for 15 min. The protein was transferred to new Eppendorf (EP) tube and quantified by Bradford method. The protein was separated by 10% sodium dodecyl sulphate-polya-

Table I. Primer sequences.

Gene	Forward 5′-3′	Reverse 5′-3′
GAPDH	AGTACCAGTCTGTTGCTGG	TAATAGACCCGGATGTCTGGT
miR-106a	CTTAGTGGTCTCTACTTGTT	TCACCCTCTCACAGCTTG
BMP-2	CCCACCTCTTCTAGAATCT	TATTGGACCTCGCGGTAATT
Collagen II	AGTGGGGTCTCTAGCTTGTT	CTCCCAACACAGCTTG

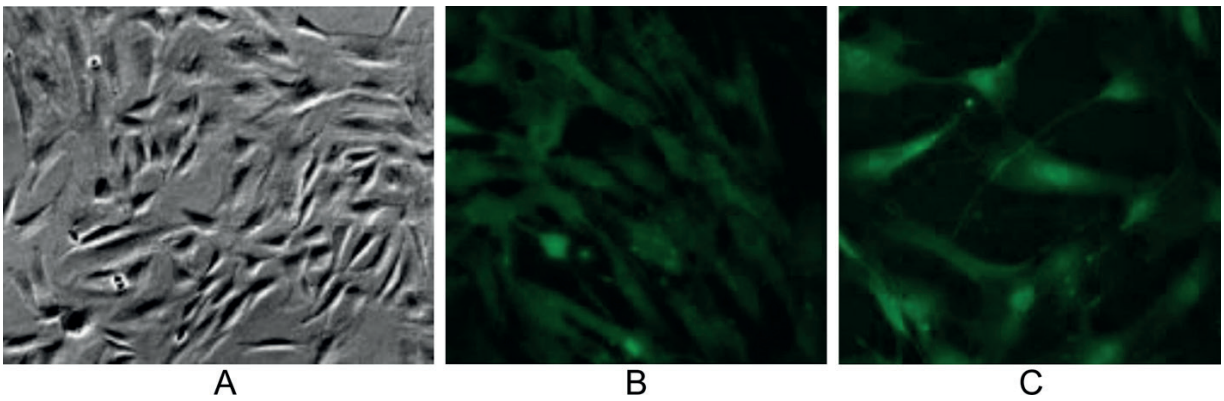

Figure 1. BMSCs isolation, morphology observation, and identification (×100). ***A,*** BMSCs morphology on the 3rd generation. ***B,*** CD29 positive; ***C,*** CD44 positive.

crylamide gel electrophoresis (SDS-PAGE) and transferred to polyvinylidene difluoride (PVDF) membrane at 100 mA for 1.5 h. After blocked by 5% skim milk for 2 h, the membrane was incubated in primary antibody (1:1000) at 4°C overnight. The membrane was incubated in goat anti rabbit secondary antibody (1:2000) at room temperature for 30 min. Next, the membrane was treated by developer for 1 min and exposed to observe the result. The film was scanned by Quantity One software (Quantity One software, Bio-Rad Laboratories, Inc. Hercules, CA, USA) and analyzed by protein image processing system. Each experiment was repeated for four times.

Statistical Analysis

All data analyses were performed on SPSS 11.5 software (SPSS Inc., Chicago, IL, USA). Measurement data were presented as mean ± standard deviation. Student's *t*-test was used to compare the differences between two groups. Tukey's post-hoc test was used to validate the ANOVA for comparing measurement data among multiple groups. $p<0.05$ was depicted as statistical significance.

Results

BMSCs Isolation and Identification in Morphology

BMSCs from primary rat exhibited suspension in round shape. After 24 h, the cells adhered in shuttle shape and grew in colony (Figure 1A). Immunofluorescence demonstrated CD29 and CD44 positive in BMSCs (Figure 1B, C).

MiR-106a Expression Analysis in BMSCs

MiR-106a expressions in BMSCs from different groups were detected. MiR-106a inhibitor transfection significantly reduced miR-106a

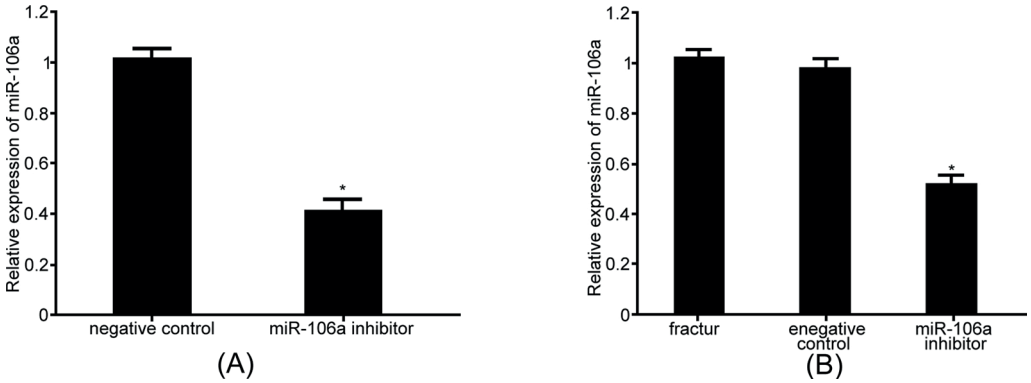

Figure 2. MiR-106a expression analysis in BMSCs. ***A,*** miR-106a expression in BMSCs. ***B,*** miR-106a expression in bone tissue. $^{*}p<0.05$, compared with negative control or fracture group.

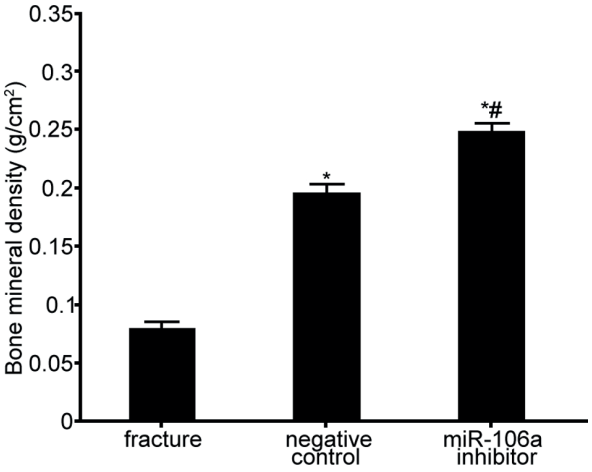

Figure 3. BMD analysis in rat after operation. $^{*}p<0.05$, compared with fracture group, $^{\#}p<0.05$, compared with negative control.

expression in BMSCs compared with negative control ($p<0.05$). Autologous oxygen release nano bionic scaffold composite miR-106a inhibitor significantly reduced miR-106a level in BMSCs compared with negative control and fracture group ($p<0.05$) (Figure 2).

General State and BMD Analysis in Rat After Surgery

Following time extension, the rat showed good recovery, normal diet and daily activity, and smooth fur without local or systemic inflammation. All the wounds healed in first intention. No significant inflammation or rejection reaction of implant materials was observed. Local bone tissue BMD was tested on 6 weeks after operation. BMD markedly increased by BMSCs treated by autologous oxygen release nano bionic scaffold composite miR-106a inhibitor group compared with fracture group ($p<0.05$). BMSCs treated by autologous oxygen release nano bionic scaffold composite miR-106a inhibitor exhibited apparently better impact on BMD compared with negative control ($p<0.05$) (Figure 3).

Serum ALP Expression in Rat

BMSCs from both autologous oxygen release nano bionic scaffold composite miR-106a inhibitor or scramble significantly increased serum ALP contents compared with fracture group ($p<0.05$). BMSCs treated by autologous oxygen release nano bionic scaffold composite miR-106a inhibitor exhibited significantly higher ALP level compared with negative control ($p<0.05$) (Figure 4).

Collagen II Expression in Rat

Real-time PCR was applied to test collagen II expression in bone tissue. BMSCs from both autologous oxygen release nano bionic scaffold composite miR-106a inhibitor or scramble significantly elevated collagen II expression in bone tissue compared with fracture group ($p<0.05$). BMSCs treated by autologous oxygen release nano bionic scaffold composite miR-

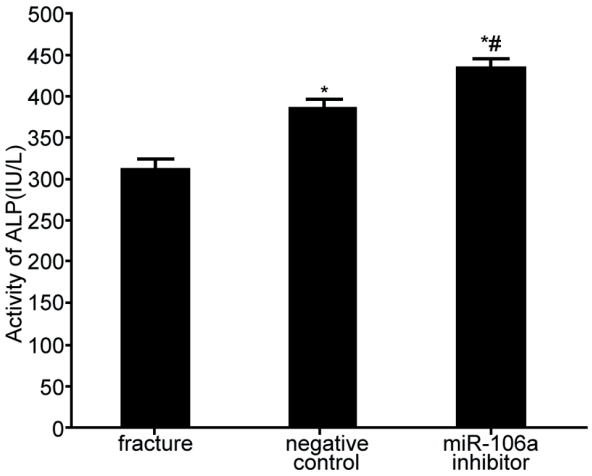

Figure 4. Serum ALP expression in rat. $^{*}p<0.05$, compared with fracture group, $^{\#}p<0.05$, compared with negative control.

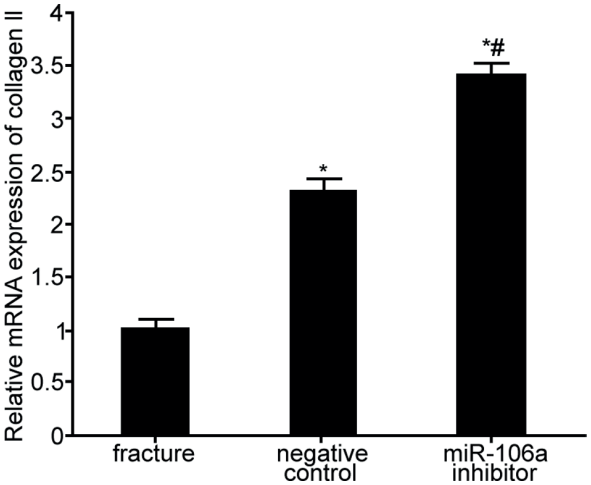

Figure 5. Collagen II expression in rat. $^{*}p<0.05$, compared with fracture group, $^{\#}p<0.05$, compared with negative control.

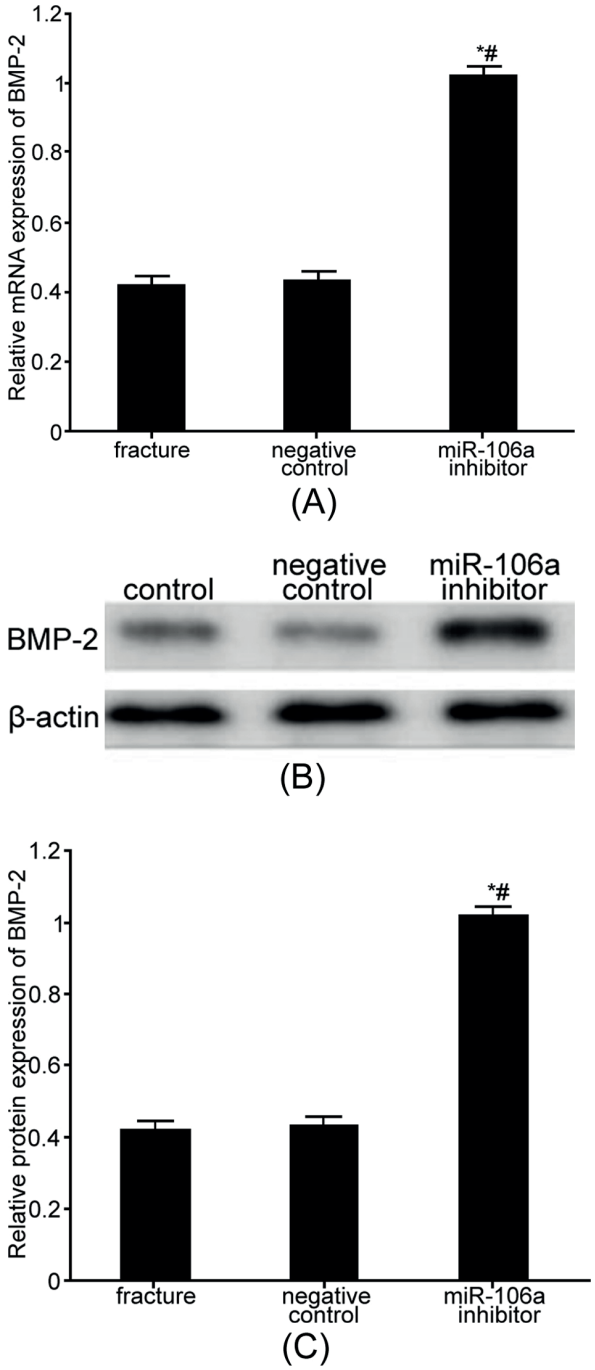

Figure 6. BMP-2 mRNA and protein expressions in rat. ***A,*** real-time PCR detection of BMP-2 mRNA expression. ***B,*** Western blot detection of BMP-2 protein expression. ***C,*** BMP-2 protein expression analysis. $^{*}p<0.05$, compared with fracture group, $^{\#}p<0.05$, compared with negative control.

106a inhibitor significantly promoted collagen II production compared with negative control ($p<0.05$) (Figure 5).

Bone Morphogenetic Protein 2 (BMP-2) mRNA and Protein Expressions in Rat

BMSCs treated by autologous oxygen release nano bionic scaffold composite miR-106a inhibitor markedly enhanced BMP-2 mRNA and protein expressions compared with fracture group and negative control ($p<0.05$) (Figure 6).

Discussion

The requirement of cell scaffold material for bone tissue construction is special in the process of the bone tissue engineering. It needs good biological compatibility to facilitate seed cell adhesion, growth, proliferation, and differentiation. In addition, its degradation product has no toxicity or teratogenic effect to the body. Moreover, it can degrade without inducing aseptic inflammation[18,19]. Researches[14,15] showed that autologous oxygen release nano bionic scaffold is featured as good mechanical property, biological activity, and auto oxygen release function, thus to promote cell adhesion, location, migration, and BMSCs osteogenesis. BMSCs were verified to have good osteogenic capability in animal models. BMSCs isolated from bone marrow can be used to repair bone defect by planting with biological active carrier hydroxyapatite and biological scaffold like tricalcium phosphate[20]. BMSCs are easy to be obtained from bone marrow, thus is worth of application in bone tissue engineering[21]. It was demonstrated[16,17] that miRNAs participate in regulating BMSCs differentiation in the process of osteogenesis. Though the role of miR-106a in BMSCs has not been reported, BMP-2 is one of its target genes[22]. BMP-2 induces MSCs osteogenic differentiation, increases osteocalcin and ALP expressions, promotes bone matrix protein expression and extracellular matrix mineralization, and facilitates osteoblast maturation[23, 24]. In this study, autologous oxygen release nano bionic scaffold composite BMSCs significantly increased local bone mineral density, promoted callus healing, facilitated ALP secretion, elevated collagen II expression, and up-regulated BMP-2 mRNA and protein levels. Autologous oxygen release nano bionic scaffold composite miR-106a induced BMSCs exhibited more significant effect on bone repair. It suggested that autologous oxygen release nano bionic scaffold composite miR-106a induced BMSCs promoted bone repair through regulating BMP-2. This work first confirmed the role of autologous oxygen release nano bionic scaffold composite miR-106a induced BMSCs in bone

repair, while its specific mechanism still needs further investigation.

Conclusions

We showed that autologous oxygen release nano bionic scaffold composite miR-106a induced BMSCs enhanced osteoblast conversion and promoted bone repair through regulating BMP-2.

Acknowledgments

This work was supported by the National Natural Science Foundation of China (No. 81201385) and the Key Project of the Medical Science and Technology Development Foundation, Nanjing Department of Health (No. YKK17062).

Conflict of Interest

The authors declare that they have no conflict of interest.

References

1) Makihara T, Yoshioka T, Sugaya H, Aoto K, Wada H, Uemura K, Tanaka K, Akaogi H, Yamazaki M, Mishima H. Feasibility and efficacy of autologous bone marrow aspirate transplantation combined with human parathyroid hormone 1-34 administration to treat osteonecrosis in a rabbit model. Bone Marrow Res 2017; 2017: 2484689.
2) Yin Z, Chen X, Song HX, Hu JJ, Tang QM, Zhu T, Shen WL, Chen JL, Liu H, Heng BC, Ouyang HW. Electrospun scaffolds for multiple tissues regeneration in vivo through topography dependent induction of lineage specific differentiation. Biomaterials 2015; 44: 173-185.
3) Chen Z, Cheng L, Feng G. Bone inflammation and chronic recurrent multifocal osteomyelitis. Eur Rev Med Pharmacol Sci 2018; 22: 1380-1386.
4) Yap CH, Park DW, Dutta D, Simon M, Kim K. Methods for using 3-D ultrasound speckle tracking in biaxial mechanical testing of biological tissue samples. Ultrasound Med Biol 2015; 41: 1029-1042.
5) Papanikolaou IG, Katselis C, Apostolou K, Feretis T, Lymperi M, Konstadoulakis MM, Papalois AE, Zografos GC. Mesenchymal stem cells transplantation following partial hepatectomy: a new concept to promote liver regeneration-systematic review of the literature focused on experimental studies in rodent models. Stem Cells Int 2017; 2017: 7567958.
6) Zhu X, Liu Z, Deng W, Zhang Z, Liu Y, Wei L, Zhang Y, Zhou L, Wang Y. Derivation and characterization of sheep bone marrow-derived mesenchymal stem cells induced with telomerase reverse transcriptase. Saudi J Biol Sci 2017; 24: 519-525.
7) Huleihel L, Sellares J, Cardenes N, Alvarez D, Faner R, Sakamoto K, Yu G, Kapetanaki MG, Kaminski N, Rojas M. Modified mesenchymal stem cells using miRNA transduction alter lung injury in a bleomycin model. Am J Physiol Lung Cell Mol Physiol 2017; 313: L92-L103.
8) Harkness L, Twine NA, Abu Dawud R, Jafari A, Aldahmash A, Wilkins MR, Adjaye J, Kassem M. Molecular characterisation of stromal populations derived from human embryonic stem cells: similarities to immortalised bone marrow derived stromal stem cells. Bone Rep 2015; 3: 32-39.
9) Kukumberg M, Yao JY, Neo DJ, Yim EK. Microlens topography combined with vascular endothelial growth factor induces endothelial differentiation of human mesenchymal stem cells into vasculogenic progenitors. Biomaterials 2017; 131: 68-85.
10) Lewandowska-Lancucka J, Fiejdasz S, Rodzik L, Koziel M, Nowakowska M. Bioactive hydrogel-nanosilica hybrid materials: a potential injectable scaffold for bone tissue engineering. Biomed Mater 2015; 10: 015020.
11) Song L, Wang S, Wang H, Zhang H, Cong H, Jiang X, Tien P. Study on nanocomposite construction based on the multi-functional biotemplate self-assembled by the recombinant TMGMV coat protein for potential biomedical applications. J Mater Sci Mater Med 2015; 26: 97.
12) Soares CJ, Castro CG, Neiva NA, Soares PV, Santos-Filho PC, Naves LZ, Pereira PN. Effect of gamma irradiation on ultimate tensile strength of enamel and dentin. J Dent Res 2010; 89: 159-164.
13) Pegado RE, do Amaral FL, Florio FM, Basting RT. Effect of different bonding strategies on adhesion to deep and superficial permanent dentin. Eur J Dent 2010; 4: 110-117.
14) Zanatta FB, Pinto TM, Kantorski KZ, Rosing CK. Plaque, gingival bleeding and calculus formation after supragingival scaling with and without polishing: a randomised clinical trial. Oral Health Prev Dent 2011; 9: 275-280.
15) Leung CC, Palomo L, Griffith R, Hans MG. Accuracy and reliability of cone-beam computed tomography for measuring alveolar bone height and detecting bony dehiscences and fenestrations. Am J Orthod Dentofacial Orthop 2010; 137: S109-S119.
16) Zhu YL, Wang S, Ding DG, Xu L, Zhu HT. miR217 inhibits osteogenic differentiation of rat bone marrowderived mesenchymal stem cells by binding to Runx2. Mol Med Rep 2017; 15: 3271-3277.
17) Zhang Y, Huang X, Yuan Y. MicroRNA-410 promotes chondrogenic differentiation of human bone marrow mesenchymal stem cells through down-regulating Wnt3a. Am J Transl Res 2017; 9: 136-145.
18) Kon E, Roffi A, Filardo G, Tesei G, Marcacci M. Scaffold-based cartilage treatments: with or without cells? A systematic review of preclinical and clinical evidence. Arthroscopy 2015; 31: 767-775.
19) Choi DJ, Choi SM, Kang HY, Min HJ, Lee R, Ikram M, Subhan F, Jin SW, Jeong YH, Kwak JY, Yoon S. Bioactive fish collagen/polycaprolactone composite na-

nofibrous scaffolds fabricated by electrospinning for 3D cell culture. J Biotechnol 2015; 205: 47-58.

20) Hosseini E, Ghasemzadeh M, Kamalizad M, Schwarer AP. Ex vivo expansion of CD3depleted cord blood-MNCs in the presence of bone marrow stromal cells; an appropriate strategy to provide functional NK cells applicable for cellular therapy. Stem Cell Res 2017; 19: 148-155.

21) Jiang XR, Yang HY, Zhang XX, Lin GD, Meng YC, Zhang PX, Jiang S, Zhang CL, Huang F, Xu L. Repair of bone defects with prefabricated vascularized bone grafts and double-labeled bone marrow-derived mesenchymal stem cells in a rat model. Sci Rep 2017; 7: 39431.

22) Fang T, Wu Q, Zhou L, Mu S, Fu Q. miR-106b-5p and miR-17-5p suppress osteogenic differentiation by targeting Smad5 and inhibit bone formation. Exp Cell Res 2016; 347: 74-82.

23) Zhang M, Bian YQ, Tao HM, Yang XF, Mu WD. Simvastatin induces osteogenic differentiatioin of MSCs via Wnt/beta-catenin pathway to promote fracture healing. Eur Rev Med Pharmacol Sci 2018; 22: 2896-2905.

24) Ramazzotti G, Bavelloni A, Blalock W, Piazzi M, Cocco L, Faenza I. BMP-2 induced expression of PLCbeta1 that is a positive regulator of osteoblast differentiation. J Cell Physiol 2016; 231: 623-629.